FUDMA Journal of Engineering and Technology
ISSN: 3092-9385
https://sites.google.com/fudutsinma.edu.ng/fjet
Volume 1, Issue 2, 2025, 97-109

Application of Upper Bound Analysis and Taguchi Method in Aluminium Extrusion

Kamardeen A. OGUNBAJO[1], Benjamin I. UGHEOKE[2], Ibrahim D. MUHAMMAD[3], Emmanuel ONCHE[4]

[1,2,3,4]Department of Mechanical Engineering, University of Abuja, Abuja, Nigeria

[1]adebayokamardeen@gmail.com, [2]ben.ugheoke@uniabuja.edu.ng, [3]d.ibrahim@uniabuja.edu.ng, [4]emmanuel.onche@uniabuja.edu.ng

Abstract

This research explores the use of upper bound analysis in calculating the extrusion force through u-shaped dies with varying fillet radii, billet lengths, friction coefficients and billet temperatures. Taguchi method was used in design of this experiment which is a four factor four level experiment giving a total of 16 experimental runs and aluminium 3003 was used as the workpiece. Based on these results a model equation was developed to predict the extrusion force. The correlation coefficient and covariance of the data generated, revealed that a positive and direct relationship existed between fillet radius, billet length, friction coefficient and extrusion force, while an inverse and indirect relationship existed between billet temperature and extrusion force. The R^2 value was 99.96% and adjusted R^2 value of 99.80% and a root mean square error of 0.2137, indicating that the accuracy of the model is good.

Keywords: *Billet lengths, billet temperatures, friction coefficients, fillet radii, Taguchi Method.*

1.0 Introduction

Extrusion can be defined as a process whereby a metal billet cross-section is reduced by applying high pressure through a die. It is used to produce regular and irregular as well as hollow shapes from materials that are soft and ductile like aluminium [1]. Extrusion is basically classified as indirect or direct depending on how the ram and billet moves (i.e. the direction). In the forward or direct extrusion, movement of the billet and punch are in the same direction as shown in Figure 1, for backward or indirect extrusion the movement of the billet and ram are in opposite directions as shown in Figure 2.

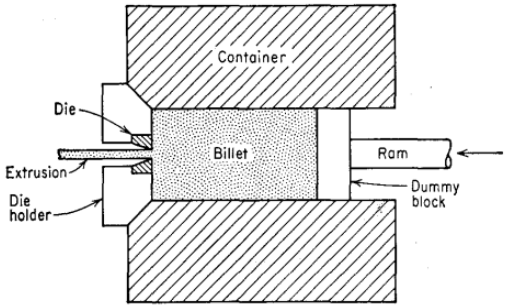

[1]

Figure 1: Direct Extrusion

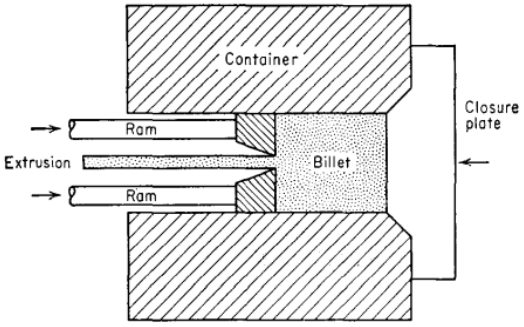

[1]

Figure 2: Indirect extrusion

This research seeks to utilize upper bound method in calculating the extrusion force required in extruding aluminium billets through u-shaped dies of varying fillet radii, billet lengths, billet temperatures and friction coefficients. Taguchi method was used in the design of experiments to obtain a set of 16 experimental runs. Taguchi method was used because it is an experimental design method which minimizes the number of

Received: 28/06/2025; Revised: 14/07/2025; Accepted: 15/07/2025; Published: 08/08/2025

experiments while providing accuracy and reliability of the process. Optimization was also done in order to determine the significant parameters as well as to determine the relationship that exists between the parameters. By this way the quality and integrity of the extrudates will be enhanced.

The paper consists of the following areas; Literature review where previous studies on related works were stated; Methodology which analysis the design equations as well explaining the design of experiment; Results which shows the performance and behaviour of the dependent variable (extrusion force), and the independent variables which are: fillet radius, billet length, billet temperature and friction coefficient and lastly a conclusion which summarizes the results of the findings. Acknowledgements and references were also duly provided.

1.1 Literature Review

A great deal of work has been carried out in the field of extrusion to study various parameters. Some of these works include:

Investigation on modelling as well as applying Taguchi and ANOVA analysis for optimizing the extrusion parameters has been studied [2]. Aluminium alloy 2A12TA was used and the chemical analyses as well as stress-strain tests were done. A finite element model was used in simulating the extrusion process thereafter analytical methods was used to validate the results, and there was good agreement between the experimental and simulated values.

Glass lubricated tube extrusion of stainless steels was simulated using a thermo-mechanical couple [3]. Extrusion problems with radial symmetry were developed in two- and three-dimension models while simulations were done using a lagragian finite element code called MSC Marc. The models were validated by comparing values of extrusion force and billet exit temperatures with values obtained experimentally from an industrial extrusion press, and there was good agreement between simulated and experimental values.

A numerical model was developed and validated to predict material flow for hot extrusion of aluminium alloy and weld formations [4]. This model successfully predicted the material flow behaviour and microstructure evolution that occurred in aluminium alloy AA3003 extrusion and it was validated against industrial data, which showed good agreement.

The various parameters affecting extrusion like speed of ram, initial temperature of the billet, as well as extrusion ratio, on the stress as well as extrusion load during the hot extrusion of Aluminium Alloy 6061was investigated [5]. Heat transfer coefficient and coefficient of friction were the design parameters considered. Container, ram, die and the billet geometries were generated in CATIA and simulation was carried out with Deform-3D software. Taguchi method was used to design a set of 16 experiments of varying extrusion variables after which input variables and output response significance was checked using ANOVA (Analysis of variance) then, the optimal parameters was determined.

AA6061—5% SiC_p composite was hot extruded and studied so as to determine the mechanical properties of extruded composite as well as the composite thermo-mechanical behaviour during the deformation [6]. Compression tests were done in order to determine its flow stress at different strain rates and temperatures. Thereafter the strain, temperature and required energy was determined using a mathematical model. Tensile and hardness tests were done so as to determine the mechanical properties of the extrudates while hot extrusion tests were also done to verify predictions derived from the model. The results obtained in both the experiments and the mathematical model showed positive agreement. The results showed that extrusion speed greatly affected mechanical properties of the extrudates.

The semi-solid extrusion of aluminium was studied [7]. It is a new process of forming which requires lower pressure to form than the conventional solid extrusion. Also, it has a low cost of production because it does not require large machines. Gas Induced Semi-Solid (GISS) process was the technique used in this study. The experiment involved injecting nitrogen gas into the molten aluminium for about 5 seconds. After which the semi-solid slurry obtained was poured in sleeve. The slurry was pushed through the extrusion die at varying speeds of 2, 4, and 6 centimetre per second by the plunger. The results revealed that holding time as well plunger speed affected the final extrudates.

Backward extrusion simulation was carried out using shapes of varying internal cross-sections like hexagonal, rectangular and elliptical as well as shapes with externally circular cross-sections. Simulation was also done for shapes that are externally circular as well as shapes that are externally polygonal and internally circular [8]. It was observed that the predicted extrusion force for lower reduction ratios agreed closely with experimental values while those for larger reduction ratios varied widely. Velocity distribution at different stages in extruding tubes of rectangular sections as well as strain, stress and load distributions tubes of hexagonal sections were obtained. It was concluded that thin walls and large reduction ratios of hollow sections are more prone to distortions as a result of differences in velocity components and different directions.

In order to obtain the optimum parameters for a two-track top profile feature angularity applicable to window assembly, aluminium alloy 6063 was hot extruded [9]. Analysis was performed with Taguchi design of experiments and S/N ratios were used to determine optimum parameters. Speed of the ram, temperature of the container and

Received: 28/06/2025; Revised: 14/07/2025; Accepted: 15/07/2025; Published: 08/08/2025

billet pre-heating temperature each with three levels were used in this study to determine the feature angularity. The optimum levels obtained were: ram speed of 6mm/sec, container temperature of 400ºC and billet pre-heating temperature of 500 ºC. Through the application of analysis of variance, speed of the ram with 59.83% contribution was the highest second was container temperature and lastly billet pre-heating temperature.

Hot metal forming processes that results in large deformations of materials was modelled and simulated using ABAQUS software [10]. The two examples used in this work are forging of steel and extrusion of aluminium alloys, and a thermoelastic visco-plasticity model was developed for each of the cases and the microstructure was also modelled effectively. Results obtained from the microstructure simulation were compared with those obtained from experiment and there was good similarity observed.

Aluminium 7005 alloy was hot compressed at strain rates of 0.001/s to 10/s and temperatures 623 K to 823 K and the results were analyzed. [11]. Aluminium 7005 alloy is being extensively used in the industry for fabrication of aircrafts and automobile components, as well as components of high-speed trains. Results indicated that decreasing deformation temperatures led to increase in strain rates as well as flow stress. Based on the true stress-strain curves, two Arrhenius-typed equations were developed with and without consideration of strain rates. Both equations adequately predicted the flow stress but equation considering the effects of strain showed more accuracy. Also, experiments were conducted and results obtained were compared with those from simulation it was observed that the behaviour of aluminium 7005 during the extrusion process was well predicted.

Extrusion of aluminium 6063 alloy to billets of circular solid profile was simulated [12]. Taguchi's orthogonal array was used in analyzing the results, analytical calculations were also done and results obtained were compared with those obtained from simulation which showed close matching.

Extrusion dies were designed for determining of process parameters in the extrusion of aluminium alloys [13]. Material properties in the Arrhenius model which considered effects of strain, as well as stress–strain parameters which were obtained from AA6N01 hot compression tests were identified using dynamic material model and the most favourable process parameters of the AA6N01 alloy were determined. The velocity uniformity was greatly improved through a series of die modification, which ensured that complex cross-section of AA6N01was successfully extruded with the required geometry and size. It was observed that there was significant agreement when experimental and numerical results were compared which verified the numerical model, the process parameters and the constitutive model.

The contact length between die and metal using local co-ordinates rotation for nodes was carried out [14]. This was used to study die length effects on relative extrusion pressure and also calculate relative extrusion pressure using varying reduction areas in ANSYS software. Contours which require less extrusion pressure and perfect die lengths were obtained.

Results of this investigation were compared with those of experiments and upper bound theory, and good agreement was obtained. Backward extrusion of AlCu5PbBi was performed to determine the extrusion force and compare results with those obtained from experiments [15]. Numerical modelling was done using ABAQUS based on finite element method, while stochastic model was done using central composite experimental design.

A coupled thermos-mechanical finite element analysis of axis-symmetric direct extrusion process of aluminium alloy was done with commercial software package ABAQUS [16]. The effects of extrusion parameters like; friction coefficient, die angle, maximum nodal temperature, die profile radius, deformation homogeneity and maximum contact pressure were studied. Heat generation due to plastic deformation and friction coefficient had little influence on deformation homogeneity and significant effect on maximum nodal temperature. Also, it was observed that the die angle has a considerable effect on contact extrusion pressure and deformation, while die profile radius had appreciable influence on contact extrusion pressure. This investigation helps in selecting appropriate process parameters for proper designing of direct extrusion process.

Linearly converging die profiles were used to numerically simulate the extrusion of advanced and simple polygons like T, L, Octagonal, Triangular etc. sections from round billets [17]. The die profiles were evaluated with mathematical equations, and the model of the converging die profile was done using Autodesk inventor while deform 3D was used for the numerical analysis of both wet and dry conditions to predict various parameters like velocity, effective stress, temperature, strain rate, and extrusion load during the deformation process. It was observed simple shapes had a lower predictive load than advanced shapes. Also, there was no significant difference between predictive loads for simple shapes with the least pressure occurring in H-sections while the highest occurs in L-section and is closely followed by T-section.

Non-steady state temperature distributions that occur in direct extrusion was simulated using a developed numerical method. [18]. Strain rates, velocity, and strain fields that occurred in the zones of deformation were derived with upper bound analytical method. Also, equations of heat transfer conduction were coupled to those of internal heat generation. The extrusion process was simulated with C++ computer programming language and factors such as friction conditions, properties of the materials, extrusion ratio, extrusion velocity, billet height, die preheat temperature, die land length and percentage reduction in area were used. The effects of percentage

Received: 28/06/2025; Revised: 14/07/2025; Accepted: 15/07/2025; Published: 08/08/2025

reduction in area and billet height on distributions of temperature inside the dead metal zone had good agreement with experimental results.

The effects of percentage reductions and frictional boundary conditions on forward extrusion of aluminium 6063 using finite element method were done. [19]. Curved die profiles of regular polygons (square, hexagonal, heptagonal, and octagonal) were designed using Autodesk Inventor 2013, while MATLAB R2009b was used to generate the coordinates as well as the model of the die from circular billet. Deform 3D was used for the simulation, while the boundary conditions were taken as 0.75 and 0.38 for dry and wet conditions respectively. The percentage reduction was varied from 50% 70% and 90%. Effective strain and stress, temperature distribution and strain rate were reported. Extrusion pressure increased with increasing die length, reduction ratio, and frictional conditions, while it decreased as the shape of polygon increased from square to hexagon and lastly octagon for both percentage reductions in area and friction factors. Also, there was no observed distinct difference between predictive loads for shaped-polygons for a given cross-sectional area and reduction ratios. Also, these results showed good agreements with those obtained experimentally from literature.

The effects of loading rate, die angle, and die reduction in area on flow patterns, extrusion pressures and quality of extrudates on cold extruded lead and aluminium alloys was investigated experimentally using four symmetrical projections with inner circular sections [20]. The average hardness values of the extrudates as well as radius of curvature for the aluminium and lead alloys increased as die reduction in area increased and also slightly increased with increasing loading rates. This shows that maximum extrusion pressures and specific coring pressures depend primarily on the loading rate, die angle and total reduction in area of the complex shaped cross section these values are a minimum at die angle of 90^{0} so as to increase die life.

An experimental investigation is done to find out how die angle affects the hardness and surface finish of cold extruded reinforced aluminium alloy [21]. The results obtained are then compared with 6061 aluminium alloy which is cold extruded. Die angles of 25^{0}, 15^{0} and 12^{0} are used. It was discovered that increased die angle led to decrease extrusion load. Also, least resistance against extrusion was observed in the 25^{0} die compared with the 12^{0} and 15^{0} dies respectively. Also increased die angle led to increased surface roughness and higher hardness values. The aluminium alloy 6061 showed lesser properties when compared to the Nano-sic aluminium alloy.

Stir casting technique was used to prepare an aluminium alloy composite matrix of AA6082 in order to investigate their mechanical properties using different percentage weight of reinforcements [22]. The mechanical properties studied include: flexural, impact, hardness and tensile values. Finite element analysis of the aluminium alloy composite matrix was performed and internal pressures were determined for different stresses. The design was done with solid works and analyzed using ANSYS after which results of stresses for steel pressure vessels and the aluminium composite matrix are compared

Warm aluminium extrusion in two dimensions was modelled using ABAQUS software [23]. The billet material was taken as Al-2014 aluminium alloy with length 75mm and diameter 40mm. Isothermal modelling was done for the extrusion (i.e. heating the billet to a certain temperature before extruding). Optimization was done for the process parameters and results indicated that larger die angles require lesser extrusion force than smaller die angles. Also, aluminium billet deformation due to compression and shearing stresses occurred in a small area. The study also indicated that, values of the stresses obtained either decrease or increase depending on length of die bearing and entrance angle of the die. In order to prevent these stresses from affecting the die, geometry, hardness and proper material selection should be done. Also, analysis was done using a 2D model of the billet and tooling which was constructed. The variables obtained include effective strain and stress as well as contact pressure and the results showed good agreement with calculated values.

The deformation behaviour and characterization of copper alloy was studied [24]. They performed studies on Copper rod extrusion. Circular copper rod of 12.5 mm diameter was extruded using the conventional extrusion machine. Microstructural investigation of the copper rods before and after the extrusion process was carried out. Hardness and tensile tests were used to determine the material properties of the extruded products. It was observed that after the extrusion process, more homogeneous and uniform grains structures were obtained. It was also discovered that the breaking load was increased by 22.9%, while the tensile strength increased by 6.8 %.

Effects of extrusion process parameters like, extrusion ratio, billet temperatures on the plastic strain and strain rate of aluminium matrix composite during hot extrusion process was investigated using Finite Element Analysis [25]. Simulation was done with ANSYS 15.0 workbench. Three extrusion ratios of 4:1, 8:1 and 15:1, and billet temperatures in the range 350 °C - 450 °C using steps of 50 °C were used in carrying out Finite Element analysis on the SiC reinforced aluminium matrix composites. Strain rates and plastic strains were found to increase with increase in the extrusion ratio. At the billet temperature of 450 °C, minimum strain rates and strains were found to occur.

Extrusion was done at optimized temperature of 450℃ for SiC particles reinforced Al matrix. The effect extrusion ratio has on surface quality and microstructure was investigated. It was observed that strain rates and plastic strains were lowest at 450℃ billet temperature and increased with increasing extrusion ratios for all

Received: 28/06/2025; Revised: 14/07/2025; Accepted: 15/07/2025; Published: 08/08/2025

temperatures. Also, higher strain rates and plastic strains occurred at 15:1 extrusion ratio and 550 ℃. Microstructural investigation showed that grain size is largely affected by strain rates. An analysis of grain size of composites which were extruded at 450℃ and the various extrusion ratios showed that optimum grain size occurred at 8:1 and higher extrusion ratio of 15:1 leads to surface cracks and hot shortness of the products. This study showed the optimum billet temperature and extrusion ration for further extrusions.

The numerical simulation for magnesium alloy pipes extrusion was studied [26]. AZ31B magnesium alloy pipes was used as the material to be extruded, while simulation was done using a finite element software ANSYS. They concluded that maximum stress of pipe must be bigger than the yield point of it in order to make the pipe extrusion, irrespective of whether the pipe was in local deformation or strengthening phase. It was also discovered that whether or not the pipe can be extruded, depends based on the ultimate strength and yield point on the true stress-strain curve of pipe.

The optimization of forward extrusion process parameters on AISI1010 and 16MnCr5 using deform3d was studied [27]. Process parameters selection so as to minimize the power consumed in extrusion was addressed. Taguchi Approach was used for optimization while simulation was done with deform 3d. The coefficient of friction, logarithmic strain and die angle were found to have the maximum impact on the extrusion force. ANOVA i.e. Analysis of variance was used to determine the optimal values of input process parameters so as to achieve minimum extrusion force. For minimum extrusion force the optimum parameters were logarithmic strain 0.3080, die angle 180 and coefficient of friction 0.080 for the two materials. The minimum extrusion force for AISI1010 was 468078 while the minimum extrusion force for 16MnCr5 is 544981. The simulated results were compared with experimental results and there was close agreement between them.

A mathematical modelling of extrusion of AA 3XXX aluminium alloy was performed [28]. The study made use of an integrated approach, consisting of, extrusion plant trials, laboratory experiments and finite element modelling for extruding AA3xxx aluminium alloy billet to I- shapes. The temperature and load were measured for microstructure analysis and model validation. Simulation was done with deform 3d. Temperature and load predictions from this model agreed well with the measured values obtained in the experimental trials.

1.2 Knowledge Gap to be filled

From literature given above, so much work has been done on extrusion parameters. But a common problem that needs to be addressed is the quality and integrity of the extrudates, some of which are bent while others are deflected. It is a common knowledge that in extrusion process, billet areas at the center moves faster than at the edges. Also, extrusion force around corners is larger than that at the center. This implies that in order to have good quality extrudates, there is need to investigate the extrusion around corners of the die, hence the reason for choosing the fillet radius as a parameter of interest. Also, friction plays a very important role in the extrusion process if the friction is too high it can lead to cracks in the extrudates, thereby making friction coefficient a parameter of interest. Billets tend to be longer after extrusion than in the initial state due to a reduction in the cross –sectional area. This justifies selecting billet length as a parameter of interest. Lastly, billet temperature was chosen as a parameter of interest because extrudates tend to flow through the dies more easily if they are hot especially if they are close to their recrystallization temperature (where change of material structures occurs due to grain refinement). Conventional dies whether conical polynomial, Bezier, or elliptical begin from circular shapes and gradually reduce to the assumed shape, this change of shape could be responsible for the bending and deflection associated with most extrudates. Hence, this research seeks to address the issues of bent and deflected extrudates by utilizing upper bound method to determine the extrusion force through u-shaped dies of varying fillet radii, billet temperatures, billet lengths and friction coefficients, through a proposed a die with similar entry and exit profile. It is hoped that by optimizing the fillet radius, the coefficient of friction, the billet temperature and billet length, better quality extrudates will be obtained.

2.0 Materials and Methods/Methodology

2.1 Upper Bound Analysis

Upper bound theorem states that the actual load required to deform a material is less than or equal to load calculated using a kinematically admissible velocity field. Upper bound analysis involves developing equations for the velocity fields and the strain rates after which the internal power of deformation, shear power, friction at punch material interface, frictional power at die-cylindrical surfaces and frictional power at fillet radius were determined. From these values, the extrusion pressure was calculated. These equations were calculated using maple software.

The assumptions used in these equations according to [29] are:

1. Longitudinal velocity v_y is equal to inlet velocity v_0 and is uniform across each material cross-section of die.
2. The yield criteria of Von-misses is applicable.
3. The rotational velocity is given by: v_x (r, x,y) = r. w (x,y)

Received: 28/06/2025; Revised: 14/07/2025; Accepted: 15/07/2025; Published: 08/08/2025

4. At the boundary defined by rotational velocity is v_x (r, x_f(y),y) and the plastic zone starts from x_f(0) and ends at x_f(y).

Assuming volume constancy of the extrusion process, $\varepsilon_r + \varepsilon_x + \varepsilon_y = 0$ (1)

$$\frac{\delta v_r\,(r,x,y)}{\delta r} + \frac{1}{r}\,v_r\,(r,x,y) + \frac{\delta v_y\,(r,x,y)}{\delta y} + \frac{1}{r}\,\frac{\delta v_x\,(r,x,y)}{\delta x} \quad (2)$$

Recall from assumption 1 above, longitudinal velocity equals inlet velocity and is uniform across each die cross section,

$$A_f\,V_f = A_0\,V_0 \quad (3)$$

$$V_{y(y)}\int_0^{x(y)} r^2{}_{(x,y)}dx = V_0\int_0^{x(0)} r^2{}_{(x,0)}dx \quad (4)$$

$$V_{y(y)} = \frac{V_0\int_0^{x(0)} r^2{}_{(x,0)}dx}{\int_0^{x(y)} r^2{}_{(x,y)}dx} \quad (5)$$

Making $\frac{\delta v_r\,(r,x,y)}{\delta r}$ subject of the formular gives

$$\frac{\delta v_r\,(r,x,y)}{\delta r} = \frac{1}{r}\,v_r\,(r,x,y) + \frac{\delta v_y\,(r,x,y)}{\delta y} + \frac{1}{r}\,\frac{\delta v_x\,(r,x,y)}{\delta x} \quad (6)$$

Collecting like terms gives

$$\frac{\delta v_r\,(r,x,y)}{\delta r} = \frac{1}{r}\{\,v_r\,(r,x,y) + r\left(\frac{\delta v_y\,(r,x,y)}{\delta y}\right) + \frac{\delta v_x\,(r,x,y)}{\delta x}\} \quad (7)$$

Integrating both sides with boundary condition at r = 0, $V_r = 0$

$$v_r\,(r,x,y) = \frac{1}{r}\int_0^r r\left[\frac{\delta v_y\,(y)}{dy} + \frac{1}{r}\,\frac{\delta v_x\,(r,x,y)}{dx}\right]\mathrm{dr} \quad (8)$$

Recall that at the start of the extrusion process, at x=0, $v_x = 0$

The next value of x component of velocity is

$$V_x\,(r,x,y) = \frac{r}{r^2{}_{(x,y)}}\int_0^x \frac{\partial}{\partial y}\left[V_{y(y)}r^2{}_{(x,y)}dx\right] \quad (9)$$

The strain rates, are given as:

$$E_{yy}\,(x,y) = \frac{\partial V y_{(y)}}{\partial y} \quad (10)$$

$$E_{rr}\,(x,y) = \frac{1}{2}\left[\frac{\partial w(x,y)}{\partial x} + \frac{\partial V_{y(y)}}{\partial y}\right] \quad (11)$$

$$E_{xx} = \frac{1}{2}\left[\frac{\partial w(x,y)}{\partial x} - \frac{\partial V y_{(y)}}{\partial y}\right] \quad (12)$$

$$E_{rx}\,(x,y) = -\frac{1}{4}\left[\frac{\partial w(x,y)}{\partial^2 x}\right] \quad (13)$$

$$E_{xy}\,(r,x,y) = \frac{r}{2}\left[\frac{\partial w(x,y)}{\partial y}\right] \quad (14)$$

$$E_{yr}\,(r,x,y) = \frac{r}{4}\left[\frac{\partial^2 w(x,y)}{\partial y \partial y} + \frac{\partial^2 v y_{(y)}}{\partial y^2}\right] \quad (15)$$

The internal power of deformation is given by:

$$W_i = r_0\iiint \sqrt{\frac{2}{3}\begin{bmatrix} E_{rr}{}^2 + E_{xx}{}^2 + E_{yy}{}^2 + \\ 2\left[E_{rx}{}^2 + E_{yx}{}^2 + E_{yr}{}^2\right] \end{bmatrix}}\,\mathrm{r\ drdxdy} \quad (16)$$

Received: 28/06/2025; Revised: 14/07/2025; Accepted: 15/07/2025; Published: 08/08/2025

The shear power is given by:

$$W_s = \frac{\sigma_0}{\sqrt{3}} \int [\Delta V]\tau_s \mathrm{ds} \tag{17}$$

$$[\Delta V]\tau_s = \sqrt{V_x\,(r,x,y)^2 + V_r\,(r,x,y)^2} \tag{18}$$

The friction at punch and material interface is given by:

$$W_1 = \frac{m\sigma_0}{\sqrt{3}} \int_0^{r_0} \int_0^{2\pi} |V_r|\, r dx dy \tag{19}$$

$$\text{Where } V_r\,(r,x,y) = \frac{-r}{2}\left[\frac{\partial v y_{(y)}}{\partial y} + \frac{\partial w_{x,y}}{\partial x}\right] \tag{20}$$

The frictional power at the work-material, and die-cylindrical surfaces is given by:

$$W_2 = \frac{m\sigma_0}{\sqrt{3}} \int_0^{H_0 - y^1} \int_0^{2\pi} V_{y(y)}\, r dx dy \tag{21}$$

Where $V_{y(y)}$ is given by:

$$V_{y(y)} = \frac{y}{H_0 - y^1} \frac{V_0 \int_0^{x(0)} r^2{}_s(x,y) dx}{\int_0^{x(y)} r^2{}_s(x,y) dx} \tag{22}$$

Consider the u-shaped die as shown in Figure 3 below:

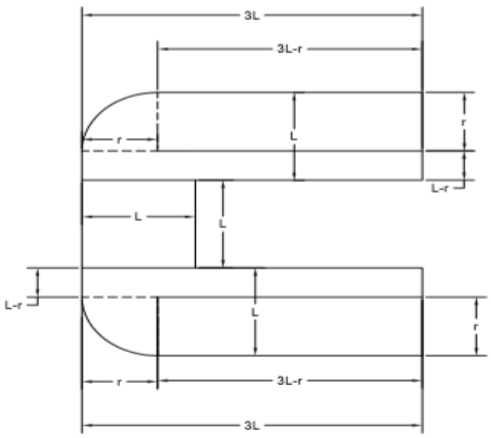

Figure 3: U shaped die

The cross-sectional area of the given U channel section =A
The two curved edges of the u-shaped die can be considered as one-quarter of the area of a circle, while the remaining parts can be considered as a rectangle.

Therefore A

$$= \frac{\pi r^2}{4} + (3l - r)r + 3l(l - r) + l^2 + 3l(l - r) + (3l - r)r + \frac{\pi r^2}{4}$$

$$\text{A} = \frac{\pi r^2}{2} + 7l^2 - 2r^2 \tag{23}$$

where r = fillet radius, and L = Length of one side of u-shaped die.
Assume die land length = x
Die angle = $\frac{\pi}{4}$
Coefficient of friction = m
Yield stress = σ_0
Applying volume constancy between entry and exit of the die, the final velocity $V_{y(y)}$is given by:

$$V_{y(y)} = \frac{V_0 \int_0^{x(0)} r^2{}_{(x,0)} dx}{\int_0^{x(y)} r^2{}_{(x,y)} dx} \tag{24}$$

Where: V_0 = initial velocity of billet

$\int_0^{x(0)} r^2{}_{(x,0)dx}$= cross-sectional area of billet before extrusion

$\int_0^{x(y)} r^2{}_{(x,y)dx}$ = cross-sectional area of billet after extrusion

Therefore the frictional power at fillet radius is given by:

$$W_3 = \frac{m* \sigma_0}{\sqrt{3}} \int_0^x \int_0^{\pi/4} V_{y(y)} r dx dy \quad (25)$$

The total frictional power is obtained by adding equations (19), (21) and (25)

$$W_T = W_1 + W_2 + W_3 \quad (26)$$

The total powers of deformation are obtained by adding equations (10), (11) and (20) gives

$$P* = W_i + W_s + W_T \quad (27)$$

The extrusion pressure is given by:

$$\frac{P}{\sigma_0} = \frac{P*}{A_0 V_0 \sigma_0} \quad (28)$$

Therefore, Extrusion Pressure $P = \frac{P*}{A_0 V_0}$ (29)

2.2 Design of Experiment and Optimization using Taguchi Method

The design of experiment was done using Taguchi Method which was generated using Minitab software. The Taguchi method involves experimental designs which are utilized for process optimization. Such designs provide accuracy to the process and reduce the number of experiments to be performed [30]. For the purpose of this study, four (4) factors and four (4) levels experimental design was used. This is because, 4 factors and 4 level design give a total of 16 experimental runs which has a wider spread and considers various experimental combinations. 2 factors and 2 levels give a total of 4 experimental runs which might not be sufficient enough to make adequate deductions, likewise 3 factors 3 levels give a total of 9 experimental runs which might also be inadequate to make adequate deductions. On the other hand, 5 factors 5 levels give a total of 25 experimental runs which might be a little too high, hence the reason for selecting 4 factors 4 levels. The levels as well as process parameters are indicated shown in the table 1 below, while the generated Taguchi Matrix is indicated at the table 2 below. The factors to be considered are: fillet radius, friction coefficient, billet temperature and billet length. Upper bound simulation was conducted for 16 runs of experiment generated by Taguchi Method after which the extrusion force was obtained

Table 1: Process parameters and corresponding levels

Process Parameters	Level 1	Level 2	Level 3	Level 4
Fillet Radius	2	4	6	8
Friction Coefficient	0.1	0.12	0.15	0.17
Billet Temperature	100	200	300	400
Billet Height	20	30	40	50

Table 2: Taguchi experimental design array

Fillet radius	Friction coefficient	Billet	Billet length
2	0.1	100	20
2	0.12	200	30
2	0.15	300	40
2	0.17	400	50
4	0.1	200	40
4	0.12	100	50
4	0.15	400	20
4	0.17	300	30
6	0.1	300	50
6	0.12	400	40
6	0.15	100	30
6	0.17	200	20

Received: 28/06/2025; Revised: 14/07/2025; Accepted: 15/07/2025; Published: 08/08/2025

Fillet radius	Friction coefficient	Billet	Billet length
8	0.1	400	30
8	0.12	300	20
8	0.15	200	50
8	0.17	100	40

3.0 Results and Discussion

Table 3: Extrusion force and signal to noise ratios

Fillet radius	Friction coefficient	Billet temperature	Billet length	Extrusion force	SNRA5
2	0.1	100	20	369491.1	111.3521
2	0.12	200	30	286736.5	109.1497
2	0.15	300	40	181553.4	105.1800
2	0.17	400	50	103107.2	100.2658
4	0.1	200	40	283938.6	109.0645
4	0.12	100	50	391044.1	111.8445
4	0.15	400	20	102405.1	100.2064
4	0.17	300	30	211147.6	106.4917
6	0.1	300	50	196841.5	105.8823
6	0.12	400	40	101686.2	100.1452
6	0.15	100	30	426445.5	112.5973
6	0.17	200	20	329670.8	110.3616
8	0.1	400	30	103977.6	100.3388
8	0.12	300	20	214979.5	106.6479
8	0.15	200	50	338259.7	110.585
8	0.17	100	40	465127.9	113.3514

Table 4: Model summary

S	R-Sq.	R-Sq. (Adj)
0.2137	99.96%	99.80%

Table 5: Analysis of variance for SN ratios

Source	DF	Seq SS	Adj SS	Adj MS	F	P
Fillet radius	3	3.337	3.337	1.112	24.35	0.013
Friction coefficient	3	1.948	1.948	0.649	14.21	0.028
Billet temperature	3	329.235	329.235	109.745	2402.39	0.000
Billet length	3	0.130	0.130	0.043	0.95	0.516
Residual Error	3	0.137	0.137	0.046		
Total	15	334.787				

Table 6: Response table for signal to noise ratios

Level	Fillet radius	Friction coefficient	Billet temperature	Billet length
1	106.5	106.7	112.3	107.1
2	106.9	106.9	109.8	107.1
3	107.2	107.1	106.1	106.9
4	107.7	107.6	100.2	107.1
Delta	1.2	1.0	12.0	0.2
Rank	2	3	1	4

Received: 28/06/2025; Revised: 14/07/2025; Accepted: 15/07/2025; Published: 08/08/2025

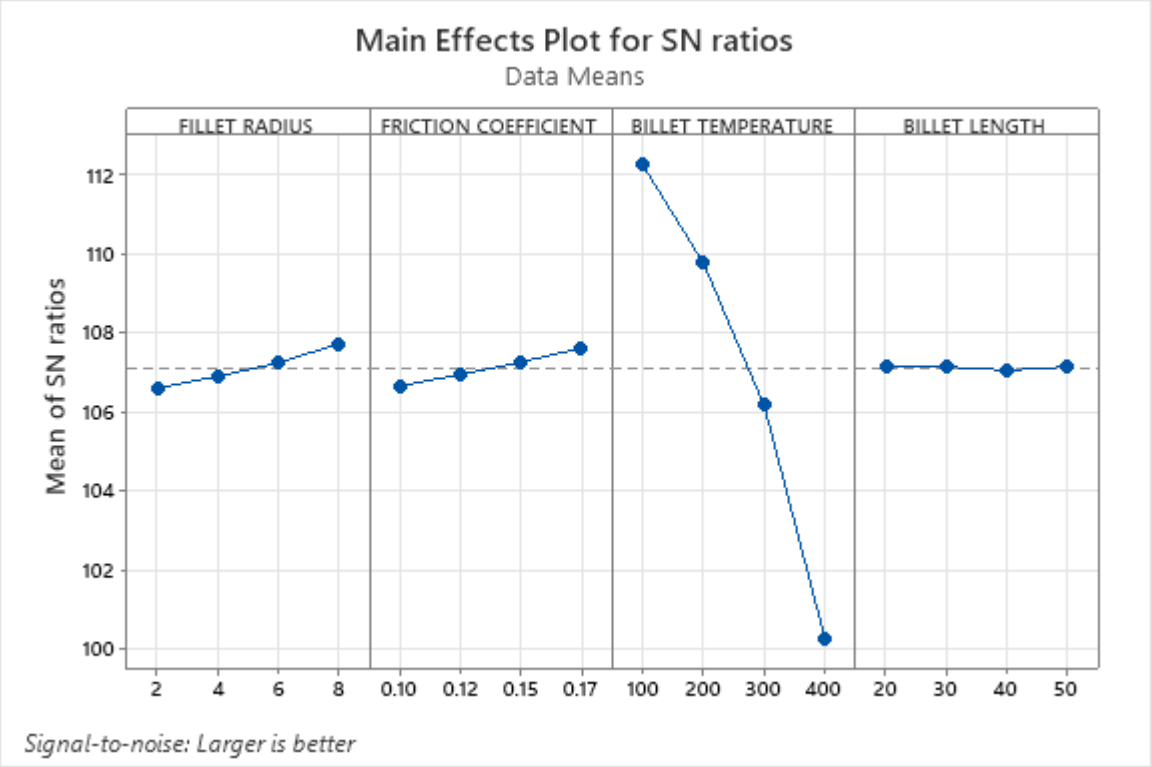

Figure 4: Main effects plots for signal to noise ratios

Table 7: Correlation coefficient

	Fillet radius	Friction coefficient	Billet temperature	Billet length
Friction coefficient	0.000			
Billet temperature	0.000	-0.000		
Billet length	0.000	0.000	0.000	
Extrusion force	0.137	0.126	-0.982	0.012

Table 8: Covariance table

	Fillet radius	Friction coefficient	Billet temperature	Billet length
Fillet radius	5			
Friction coefficient	0	0		
Billet temperature	0	-0	13333	
Billet length	0	0	0	133
Extrusion force	38599	426	-13821280	17538

Table 9: Regression equation

Extrusion force	= 407879 + 7426 fillet radius + 512136 friction coefficient - 1059.4 billet temperature + 238 billet length

Table 10: Validation results

Fillet radius	Friction coefficient	Billet temperature	Billet length	Extrusion force	Validation Results	% error
2	0.1	100	20	369491.1	372764.6	-0.89
2	0.12	200	30	286736.5	279447.3	2.54
2	0.15	300	40	192050.2	191251.4	0.41
2	0.17	400	50	103107.2	97934.12	5.02
4	0.1	200	40	283938.6	286436.6	-0.88

Received: 28/06/2025; Revised: 14/07/2025; Accepted: 15/07/2025; Published: 08/08/2025

Fillet radius	Friction coefficient	Billet temperature	Billet length	Extrusion force	Validation Results	% error
4	0.12	100	50	391044.1	404999.3	-3.57
4	0.15	400	20	102405.1	95403.4	6.84
4	0.17	300	30	211147.6	213966.1	-1.33
6	0.1	300	50	196841.5	197728.6	-0.45
6	0.12	400	40	101686.2	99651.32	2.00
6	0.15	100	30	426445.5	430455.4	-0.94
6	0.17	200	20	329670.8	332378.1	-0.82
8	0.1	400	30	103977.6	101880.6	2.02
8	0.12	300	20	214979.5	215683.3	-0.33
8	0.15	200	50	338259.7	344127.4	-1.73
8	0.17	100	40	465127.9	457930.1	1.55

3.1 Discussion of Results

Table 3 shows the calculated results from the upper bound method as well as the signal to noise ratios, Table 4 shows the model summary, and the R^2 value is 99.96% while the R^2(Adj) value is 99.8% indicating that the accuracy of the model is good. Table 5 shows the significant parameters affecting the extrusion in this study is the billet temperature since it has a p value of 0.001, which is less than 0.05, followed by fillet radius with a p value of 0.013 and then friction coefficient with a p value of 0.028. Table 6 gives the response table indicating that the parameter that contributes most to the model is the billet temperature, followed by fillet radius, then friction coefficient, and lastly billet length.

Figure 4 shows the main effects plots for the signal to noise ratios, indicating that the maximum extrusion force occurs at fillet radius 8mm, friction coefficient 0.17, billet temperature 100 ^{o}C and billet length 50mm. The minimum extrusion force was found to occur at fillet radius 2mm, friction coefficient 0.1, billet temperature 400^{o}C and billet length 20mm. Table 7 shows the correlation coefficient which measures the strength and direction of the linear relationship between two variables. It shows that a positive (direct) correlation exists between fillet radius, friction coefficient, billet length and extrusion force, while a negative (inverse) correlation exists between the extrusion force and billet temperature.

Table 8 shows the covariance table which indicates how much two variable change together. It indicates that as the fillet radius, friction coefficient and billet length increase, the extrusion force also increases and vice versa. It also indicates as the billet temperature increases, the extrusion force reduces and vice versa. Table 9 gives the regression equation which was developed to adequately predict the extrusion force, the root mean square error "S" was found to be 0.2137.

Table 10 shows the validation results which was obtained by solving the model equation generated and imputing the variables. The percentage error is also indicated.

4.0 Conclusions

This research presents the application of upper bound method in the calculation of extrusion force using a four factor four level experimental design. The deisgn of experiment was done using Taguchi method, in which a set of 16 equations were generated. A model equation was developed which predicted extrusion force. The covariance and correlation coefficients showed a positive direct relationship between fillet radius, billet length, friction coefficient and extrusion force, and an inverse/negative relationship between the extrusion force and billet temperature. This is as a result of the aluminium becoming softer at higher temperatures hence a lower extrusion force is needed. The model equation was validated by imputing the extrusion parameters and the percentage error was also computed which showed minimal error.

Acknowledgements

I wish to acknowledge the contributions of Mr Nicholas Agbo of Defence Industry Corporation of Nigeria (DICON), Kaduna, Nigeria and Mr Omenka of Joseph Tarka University of Agriculture makurdi for their efforts in completing this study.

Nomenclature

r_0 = Initial radius of billet
y_1 = Die length
v_y = Longitudinal velocity
v_0 = Inlet velocity

v_r = Rotational velocity
$x_f(0)$ = Beginning of plastic zone of deformation
x_f (y) = End of plastic zone of deformation
r = Final radius of Extrudates
v_x = Radial velocity
E_{rr} , E_{xx} , E_{yy} , E_{rx} , E_{xy} , E_{yr} = Strain rate components
W_i = Internal power of deformation
W_s = Shear power
W_1 = Friction at punch and material interface
W_2 = Frictional power at the work-material, and die-cylindrical surfaces
m = Friction coefficient
H_0 = Initial billet height
y^1= Current billet height
σ_0 = Yield strength
W_3 = Frictional power at fillet radius
A = Die cross-sectional area
r = Fillet radius
L = Length of one side of u-shaped die
x = Die land length
W_T = Total frictional power
P^* = Total power of deformation
P = Extrusion pressure

References

[1] Dieter, G., E. (1986). Mechanical Metallurgy. S.I. Metric Edition, McGraw Hill book Company, 616-617.
[2] Hosseini, A., Farhangdoost, K., H, & Manoochehri, K. (2012). Modelling of Extrusion Process and Application of Taguchi Method and ANOVA Analysis for Optimization of the Parameters. Mechanika, 18(3), 301-305.
[3] Hanson, S., & Domkin, K. (2005). Physically Based Material Model in Finite Element Simulation of Extrusion of Stainless Steel Tubes. Conference Proceedings of the 8th International Conference on Technology of Plasticity (ICTP), Verona Italy, 1-8.
[4] Mahmoodkhani, Y., Wells, M., Parson, N., & Poole, W., J. (2014). Numerical Modelling of the Material Flow during Extrusion of Aluminium Alloys and Transverse Weld Formation. Journal of materials Processing Technology, DOI: 10.1016/j.jmatprotec.2013.09.028, 214(3): 688-700.
[5] Ramya, K., & Sreedevi, K. (2016). Modelling and Optimization of Extrusion Process Parameters of AA6061 using Taguchi Method. International Journal of Engineering and Technology, 03(08), 1753-1756.
[6] Akhgar, J., M., & Mirjalili, A., S. (2011). An Investigation into the Deformation Behaviour of AA6061-5%SiCp Composite during and after Hot Extrusion Process. Proceedings of Institute of Mechanical Engineering L.J Mater des Appl, 225(1) 22-31.
[7] Rattanochaikal, T., Janudom, S., Memongkol, N., & Wannasin, J. (2010). Development of Aluminium Semi-Solid Extrusion Process. Journal of Materials and Minerals, 20, 17- 21.
[8] Arbinia, K., & Orangi, S. (2010). Numerical Study of Backward Extrusion Process Using Finite Element Method. Finite Element Analysis, David Moratal Intech Open DOI: 10 5772/10219, 381-400.
[9] Chahure, A., S., & Inamdar, K., H. (2017). Optimization of Aluminium Extrusion Process using Taguchi Method. IOSR Journal of Mechanical and Civil Engineering, 61-65.
[10] Parvizian, F., Schneidt, A., Svendsen, B., & Mahnken, R. (2010). Thermo-Mechanically Coupled Modelling and Simulation of Hot Metal Forming Processes Using Adaptive Remeshing Method. GAMM- MiH DOI 10:1002/gamm, 201010008, 33(1), 95- 115.
[11] Chen, L., Zhao, G., Yu, J., & Zhang, W. (2010). Constituted Analysis of Homogenized 7005 Aluminium Alloy at Elevated Temperatures for Extrusion Processes. Mater des 2015: 66:129-136.
[12] Kapadia, N., & Desai, A. (2015). Review on Optimization Study of Die Extrusion Process Using Finite Element Method. International Journal of Scientific Research Development, (392), 2328-2330.
[13] Dang, Y., Y., Zhang, C., S., Zhao, G.,Q., Guan, Y., J., Gao, A., J., & Sun, W., C. (2016). Constitutive Equations and Processing maps of an Al-Mg-Si Aluminium Alloy. Determination and Application in Simulating Extrusion Process of Complex Profiles. Materials & Design, 92, 983-997.
[14] Jabar, K., J. (2010). Calculation of Relative Extrusion Pressure for Circular Section by Local Co-ordinates System Using Finite-Element Method. Diyala Journal of Engineering Sciences, 03, (2) 80-96.

Received: 28/06/2025; Revised: 14/07/2025; Accepted: 15/07/2025; Published: 08/08/2025

[15] Barisic, B., Car, Z., & Ikoric, M. (2008). Analysis of Different Modelling Approach of Determining Backward Extrusion Force on AlCu 5PbBi Material. Metallurgia, 313-316.
[16] Yadav, R., R., Dewang, V., Raghuwonshi, J., & Sharma, V. (2018). Finite Element Analysis of Extrusion Process Using Aluminium Alloys. Materials Today Proceedings, Elsevier, 24, 500- 509.
[17] Oyinbo, S., T., Ikumapayi, O., M., Ajiboye, J., S., & Afolalu, S., A. (2015). Numerical Simulation of Axisymmetric and Asymmetric Extrusions Process using Finite Element Method. International Journal of Scientific and Engineering Research, 6(6), 1245-1259.
[18] Ajiboye, J., S., & Adeyemi, M., B. (2008). Effects of Extrusion Variables on Temperature Distribution in Axisymmetric Extrusion Process, International Journal of Mechanical Sciences, SO (3): 522-537, DOI: 10.1016/jijmecsci-2007.08.006,
[19] Oyinbo, S., T., Jen, C., T., & Ismail, S., O. (2020). Effects of Frictional Boundary Conditions and Percentage Area Reduction on the Extrusion Pressure. Engineering Solid Mechanics, 8(2020) 205-214.
[20] Onuh, S., O., Ekoja, M., & Adeyemi, M., B. (2003). Effects of Die Geometry and Extrusion Speed on the Cold Extrusion of Aluminium Alloy. Journal of Materials Processing Technology, DOI: 10.1016/50924 0136(02) 00941-X, 132 (1-3): 274-285.
[21] Kumar, A., V., Ratnam, C., H., Kesava -Rao, V., S., & Kumar, C., R. (2019). Study on Influence of Die Angle in Cold Extrusion on Properties of Nano Sic Reinforced 6061 Aluminium Alloy. Materials Today Proceedings, 18(7), 4366-4373.
[22] Mohammed, V., Prasath, S., Arunkumar, M., Pradeep, G., M., & Babu, S., S. (2021). Modelling and Stress Analysis of Aluminium Alloy Based Composite Pressure Vessel through ANSYS Software. Materials Today Proceedings, 37(2), 1911-1916.
[23] Magid, H., M., Sulaiman, S., & Ariffin, M., K., A. (2014). Modelling and Simulation of Forward Al- Extrusion Process using FEM. Applied Mechanics Material, Trans Tech Publications, Switzerland, Doi:1010.4028/www.scientific.net/Amm.564.525, 64, 525-532.
[24] Shalini, K., Ajeet, K., R., Devendra, K., U., & Rahul, C., F. (2015). Deformation Behaviour and Characterization of Copper Alloy in the Extrusion Process. International Journal of Mechanical Engineering Technology (IJMET), IAEME Publication, 6(7), 72-78.
[25] Dhanalakshmi, S., Svakumar, P., Shanmuga, K., S., & Arand, S. (2017). Finite Element Analysis and Experimental Study on Effects of Extrusion Ratio during Hot Extrusion Process of Aluminium Matrix Composites. Defence Science Journal, DOI: 1014429/dsj67.11535, 67(4), 428-436.
[26] Daiquan, Z., & Guoping, C. (2012). The Numerical Simulation for Extrusion Forging of Magnesium Alloy Pipes. International Conference on Solid State Devices and Materials Elsevier Physics Proceedings, 25, 125-129.
[27] Fancy, K., A., SrinivasaRao, C., & Gopalarishnaiah, P. (2018). Optimization of Direct Extrusion Process Parameter on 16MnCr5 and AISI 1010 using Deform 3D. 14th Global Congress on Manufacturing and Management Elsevier Procedia Manufacturing, 30, 498-505.
[28] Yahya, M., Many, A., W., Nick, P., Yuanyuan, G., & Warren, J., P. (2010). Mathematical Modelling on the Extrusion of AA3xxx Aluminium Alloys. Proceedings of the 12th International Conference on Aluminium Alloys, Yokohama Japan, 566-571.
[29] Ajiboye, J., S., & Adeyemi, M., B. (2007). Upper Bound Analysis for Extrusion at Various Die Land Lengths and Shaped Profiles. International Journal of Mechanical Sciences, Elsevier, 49, 335-351.
[30] Jude, A., O., Emmanuel, I., E., Sonal, N., Daniele, C., Ajay, K., D., & Janusz, A., K. (2021). Modelling and Process Optimization of Hydrothermal Gasification for Hydrogen Production A Complete Review. Journal of Supercritical Fluids, 173, 105199 https: doi.org/10.1016/j. supflu.2021.105199.

Received: 28/06/2025; Revised: 14/07/2025; Accepted: 15/07/2025; Published: 08/08/2025